Bioorganic Chemistry 38 (2010) 37–41

Contents lists available at ScienceDirect

Bioorganic Chemistry

journal homepage: www.elsevier.com/locate/bioorg

L-Glyceraldehyde 3-phosphate reductase from *Escherichia coli* is a heme binding protein

Kevin K. Desai, Brian G. Miller *

Department of Chemistry and Biochemistry, Florida State University, Tallahassee, FL 32306-4390, United States

ARTICLE INFO

Article history:
Received 29 September 2009
Available online 26 November 2009

Keywords:
Kvβ
L-Glyceraldehyde 3-phosphate reductase
Gpr
YghZ
Heme

ABSTRACT

Recently, we reported that YghZ from *Escherichia coli* functions as an efficient L-glyceraldehyde 3-phosphate reductase (Gpr). Here we show that Gpr co-purifies with a *b*-type heme cofactor. Gpr associates with heme in a 1:1 stoichiometry to form a complex that is characterized by a K_d value of 5.8 ± 0.2 μM in the absence of NADPH and a K_d value of 11 ± 1.3 μM in the presence of saturating NADPH. The absorbance spectrum of reconstituted Gpr indicates that heme is bound in a hexacoordinate low-spin state under both oxidizing and reducing conditions. The physiological function of heme association with Gpr is unclear, as the L-glyceraldehyde 3-phosphate reductase activity of Gpr does not require the presence of the cofactor. Bioinformatics analysis reveals that Gpr clusters with a family of putative monooxygenases in several organisms, suggesting that Gpr may act as a heme-dependent monooxygenase. The discovery that Gpr associates with heme is interesting because Gpr shares 35% amino acid identity with the mammalian voltage-gated K^+ channel β-subunit, an NADPH-dependent oxidoreductase that endows certain voltage-gated K^+ channels with hemoprotein-like, O_2-sensing properties. To date the molecular origin of O_2 sensing by voltage-gated K^+ channels is unknown and the results presented herein suggest a role for heme in this process.

1. Introduction

YghZ, herein referred to as L-glyceraldehyde 3-phosphate reductase (Gpr), was recently identified following a genetic selection for *Escherichia coli* genes capable of restoring the growth of a triosephosphate isomerase (TIM) deficient bacterium under gluconeogenic conditions [1]. Subsequent characterization of Gpr demonstrated that the enzyme provides a bypass of the TIM reaction by catalyzing the stereospecific, NADPH-dependent reduction of L-glyceraldehyde 3-phosphate (L-GAP) to form L-glycerol 3-phosphate. The magnitude of the second-order rate constant of L-GAP reduction by Gpr is $4.2 \times 10^5\ M^{-1}\ s^{-1}$, indicating that L-GAP may be the physiological substrate for the enzyme. L-GAP, however, is not recognized as a natural metabolite and the extent to which this compound is produced and/or accumulates in living organisms is unknown [2]. Nevertheless, the finding that L-GAP inhibits a number of enzymes including L-glyceraldehyde 3-phosphate acyltransferase, phosphatidylglycerol phosphate synthase and aldolase provides a rationale for the existence of an *in vivo* mechanism for L-GAP removal [3,4].

Gpr is a member of the aldo–keto reductase superfamily (AKR), a group of $(\beta/\alpha)_8$-barrel enzymes that act upon a broad range of aldehyde and ketone substrates [5]. The best characterized homologue of Gpr is the mammalian β-subunit of the voltage-gated K^+ channel (Kvβ), which shares 35% amino acid identity with Gpr (Fig. 1). Kvβ subunits form a permanent complex on the cytoplasmic face of many Kv channels and modulate their function [6,7]. Kvβ has been shown to be an active AKR and oxidation of the NADPH cofactor has been linked to channel modulation [8,9]. A role for Kvβ in O_2 sensing has also been postulated based on the finding that Kvβ1.2 confers Kv4.2 with hemoprotein-like, O_2-sensing properties [10]. To date, the identity of the O_2 sensory component of fully assembled voltage-gated K^+ channels remains unknown. Here we demonstrate that Gpr, the bacterial homologue of Kvβ, is a heme binding protein.

2. Materials and methods

2.1. Extraction and mass spectrometry of heme

Heme was extracted using 2% HCl in acetone [11]. Protein was subsequently removed by centrifugation and the supernatant

Abbreviations: Gpr, L-glyceraldehyde 3-phosphate reductase from *Escherichia coli*; L-GAP, L-glyceraldehyde 3-phosphate; AKR, aldo–keto reductase; Kvβ, voltage-gated potassium channel β-subunit; MALDI, matrix-assisted laser desorption/ionization; HO-1, heme oxygenase 1; ChuX, *E. coli* heme utilization protein X; IsdI and IsdG, iron-regulated surface determinant I/G.

* Corresponding author. Address: 217 Dittmer Laboratory of Chemistry, Department of Chemistry and Biochemistry, Florida State University, Tallahassee, FL 32306-4390, United States. Fax: +1 850 644 8281.
E-mail address: miller@chem.fsu.edu (B.G. Miller).

0045-2068/$ - see front matter © 2009 Elsevier Inc. All rights reserved.
doi:10.1016/j.bioorg.2009.11.003

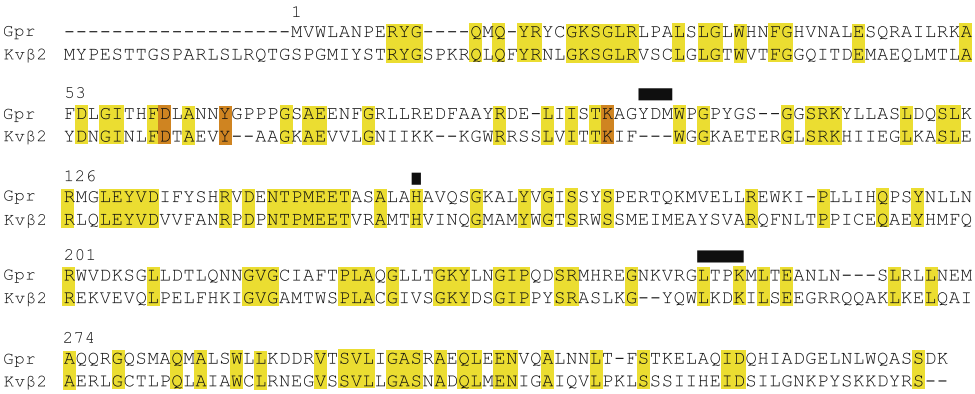

Fig. 1. Amino acid alignment of *E. coli* Gpr with *Homo sapien* Kvβ2. Regions of identity are highlighted in yellow and catalytic residues are shown in orange. Alignment was constructed using the program CLUSTALW with minor adjustments based upon visual inspection. Gpr variants constructed in this study are indicated with black boxes over the amino acids that were deleted or mutated (For interpretation of the references to color in this figure legend, the reader is referred to the web version of this article.).

was mixed 1:1 with a MALDI matrix solution (10 mg/mL α-cyano-4-hydroxycinnamic acid in 50% acetonitrile/0.1% trifluoroacetic acid) and spotted onto a MALDI target plate. Spectra were acquired on a Shimadzu Axima CFR plus in positive reflectron mode.

2.2. Cloning, expression and purification of C-terminal strep-tagged Gpr

Gpr was PCR amplified from genomic DNA isolated from *E. coli* strain MG1655 and cloned between the NcoI and BamHI sites of pET15. *Gpr* was amplified using the following primers: forward 5′-TAT CCA TGG TCT GGT TAG CGA ATC C-3′ and reverse 5′-ATG GAT CCT CAT TTT TCA AAC TGT GGA TGG CTC CAA GCT TTA TCG GAA GAC GCC TGC C-3′. These primers add a strep tag to the C-terminus of *gpr* consisting of the amino acids; ala, trp, ser, his, pro, gln, phe, glu and lys. Clones were verified by sequencing and transformed into BL21(DE3). For protein production, cultures were grown in LB containing ampicillin (100 μg/mL) at 37 °C to an OD of ~0.8 at 600 nm. IPTG was added to 0.75 mM and growth was continued for 2 h. Bacteria were collected by centrifugation and resuspended in 8 mL per gram of wet cell pellet with lysis buffer (50 mM sodium phosphate pH 7.5, 0.3 M NaCl). Cell extracts were prepared by passage through a French pressure cell at 18,000 psi. Cell lysate was cleared by centrifugation for 1 h at 30,000*g* and loaded onto a 5 mL StrepTrap column (GE Healthcare). The column was washed with 50 mL of lysis buffer and eluted with lysis buffer containing 2.5 mM desthiobiotin. Purified Gpr was exchanged into 100 mM sodium phosphate pH 7.3 containing 100 mM NaCl using 2 × 5 mL HiTrap desalting columns (GE Healthcare). The concentration of Gpr was determined from absorbance readings at 280 nm using a calculated extinction coefficient of 64,985 M^{-1} cm^{-1} (ExPASy).

2.3. Determination of the dissociation constant for heme binding to Gpr

A hemin solution (2 mM hemin chloride dissolved in 0.1 M NaOH, 5% dimethylsulfoxide, 0.2 μm filtered) was simultaneously titrated into a solution of 8 μM C-terminal strep-tagged Gpr in buffer (0.1 M sodium phosphate pH 7.3, 0.1 M NaCl) and a reference cuvette containing buffer only. The concentration of the heme solution was determined spectroscopically (ε_{385} = 58.4 mM^{-1} cm^{-1}) [12]. Prepared heme was kept in the dark on ice and used within 3 h. Difference absorbance spectra were recorded 3 min after heme was added to Gpr. After a 3 min equilibration time at 25 °C there were no further changes in the Gpr–heme spectrum. The data from the difference absorption spectra of heme titrations were plotted and fit to a one-binding site equation; $EL = 0.5(E_0 + L_0 + K_d - ((E_0 + L_0 + K_d)^2 - 4E_0 \times L_0)^{1/2})$ [13], where $\Delta A = \Delta\varepsilon \times EL$ and ΔA is the absorbance difference between sample and reference cuvettes; $\Delta\varepsilon$ is the difference extinction coefficient between bound and free heme; EL is the concentration of Gpr–heme complex; L_0 is the total heme concentration; and K_d is the dissociation constant. The K_d values reported in the text are the mean values obtained from two separate heme titration experiments. Each replicate was performed with freshly prepared C-terminal strep-tagged Gpr. The error reported indicates the deviation from the mean.

2.4. Extinction coefficient calculation of the Soret peak

The extinction coefficient of the Soret peak was calculated by taking the ΔA_{414} maximum from the difference spectrum, in the absence of NADPH, and adding the absorbance value of 8 μM free heme obtained from the reference titration. This value was then divided by the concentration of Gpr present (8 μM). The extinction coefficients obtained from two separate heme titration replicates were averaged to obtain a value of 131 mM^{-1} cm^{-1}.

2.5. Reductase activity assays of human N-terminal truncated Kvβ2

Human Kvβ2 (Accession # BC126424) encoding amino acids 36-367 was cloned into pET22(b) such that a hexahistidine tag was added to the C-terminus. Kvβ2 was expressed in BL21(DE3) by growing cultures at 37 °C in LB containing ampicillin (100 μg/mL) to an OD of 1.4 at 600 nm. IPTG was then added to 0.5 mM, the temperature was reduced to 20 °C and growth was continued for 16 h. The cell pellet was resuspended in 8 mL per gram of wet pellet weight with lysis buffer (20 mM Tris pH 7.7, 0.3 M NaCl, 40 mM imidazole). Cell extracts were prepared by passage through a French pressure cell at 18,000 psi. Cell lysate was cleared by centrifugation for 1 h at 30,000*g* and loaded onto a 5 mL Ni^{2+}–NTA affinity column (GE Healthcare). The column was washed with 50 mL of lysis buffer and then 50 mL of lysis buffer containing 70 mM imidazole. Pure protein was eluted with lysis buffer containing 250 mM imidazole and dialyzed overnight against 20 mM Tris pH 8.0, 150 mM KCl. The concentration of hexahistidine-tagged Kvβ2 was determined from absorbance readings at 280 nm using a calculated extinction coefficient of 62,130 M^{-1} cm^{-1} (ExPASy). The single-turnover catalytic activity of hexahistidine-tagged Kvβ2 was assayed by monitoring the decrease in absorbance of bound NADPH at 363 nm in a 1 mL reaction at 25 °C. The reaction buffer was 20 mM Tris pH 8.0 and 150 mM KCl.

2.6. Heme titration with human Kvβ2

Kvβ2, encoding amino acids 36-367, was PCR amplified from cDNA (Accession # BC126424) with primers that add a streptavidin affinity tag to the C-terminus and this construct was cloned into pET22(b). Kvβ2 was expressed in BL21(DE3) as described for the hexahistidine tagged construct. Kvβ2 was purified and heme titrations were performed with 8 μM Kvβ2 as described for Gpr. The concentration of Kvβ2 was determined from absorbance readings at 280 nm using a calculated extinction coefficient of 67,630 M^{-1} cm^{-1} (ExPASy).

3. Results

3.1. Characterization of heme-bound Gpr

We discovered that Gpr present in *E. coli* whole cell lysates co-purifies with a *b*-type heme. In a large-scale growth of *E. coli* strain BW25113 harboring the Gpr-encoding ASKA clone [14], we observed that N-terminal hexahistidine tagged Gpr displayed a yellow–brown color following elution from a Ni^{2+}–NTA affinity column. The absorbance spectrum of the protein measured in the presence of elution buffer (20 mM Tris pH 7.7, 0.3 M NaCl, 0.25 M imidazole) revealed maxima at 412, 528, and 564 nm under oxidizing conditions (Fig. S1). Upon addition of the reducing agent dithionite, these peaks shifted to 426, 528, and 559 nm, respectively. This absorbance spectrum is characteristic of a heme cofactor [15]. To identify the chemical identity of the bound heme, the prosthetic group was extracted from the Gpr preparation with acidic acetone [11]. The mass spectrum revealed a mass of 616.5 Da, which corresponds to the expected mass of a *b*-type heme (616.8 Da) (Fig. S2).

To investigate the stoichiometry and binding affinity of Gpr for heme, the protein was produced and purified in the absence of the hexahistidine tag encoded by the ASKA clone to prevent nonspecific heme association. Purified C-terminal strep-tagged Gpr was readily reconstituted with heme under oxidizing conditions. Difference absorbance spectra were recorded at varying heme concentrations to reveal absorbance maxima at 414, 533 and 560 nm (Fig. 2a). A heme-binding curve was generated by plotting $\Delta A_{414\ nm}$ obtained from the difference absorbance spectrum against heme concentration (Fig. 2b). The binding curve demonstrated that Gpr binds heme in a 1:1 stoichiometry. To measure heme binding affinity, the titration data were fit to a one-binding site quadratic equation [13] to estimate a K_d of 5.8 ± 0.2 μM in the absence of NADPH and a K_d of 11 ± 1.3 μM in the presence of saturating NADPH (150 μM). The heme titration difference absorbance spectrum in the presence of 150 μM NADPH had absorbance maxima identical to those obtained in the absence of cofactor (Fig. S3). The heme affinity of Gpr is similar to that reported for other hemoproteins including HO-1 (0.84 ± 0.2 μM) [16], ChuX (1.99 ± 0.02 μM) [17], IsdI (3.5 ± 1.4 μM) and IsdG (5.0 ± 1.5 μM) [18]. Using the $\Delta A_{414\ nm}$ maximum of the Soret peak from the difference spectrum and dividing it by the concentration of Gpr present (8 μM), the extinction coefficient was measured to be 131 mM^{-1} cm^{-1}. The magnitude of the Soret peak extinction coefficient of Gpr is also similar to that for other characterized hemoproteins [18]. The effect of heme on the steady-state kinetics of L-GAP reduction by Gpr was analyzed by assaying heme reconstituted Gpr. The steady-state kinetic parameters for L-GAP reduction were nearly identical for apo and heme reconstituted Gpr (data not shown).

The absorbance spectrum of reconstituted Gpr indicates that the heme exists in a hexacoordinate low-spin state under both oxidizing and reducing conditions. The Gpr–heme complex, with free heme removed on a desalting column, revealed absorbance maxima at 412 (Soret), 528 (β) and 564 nm (α) under oxidizing conditions (Fig. 2c). The addition of dithionite reduces the iron causing a

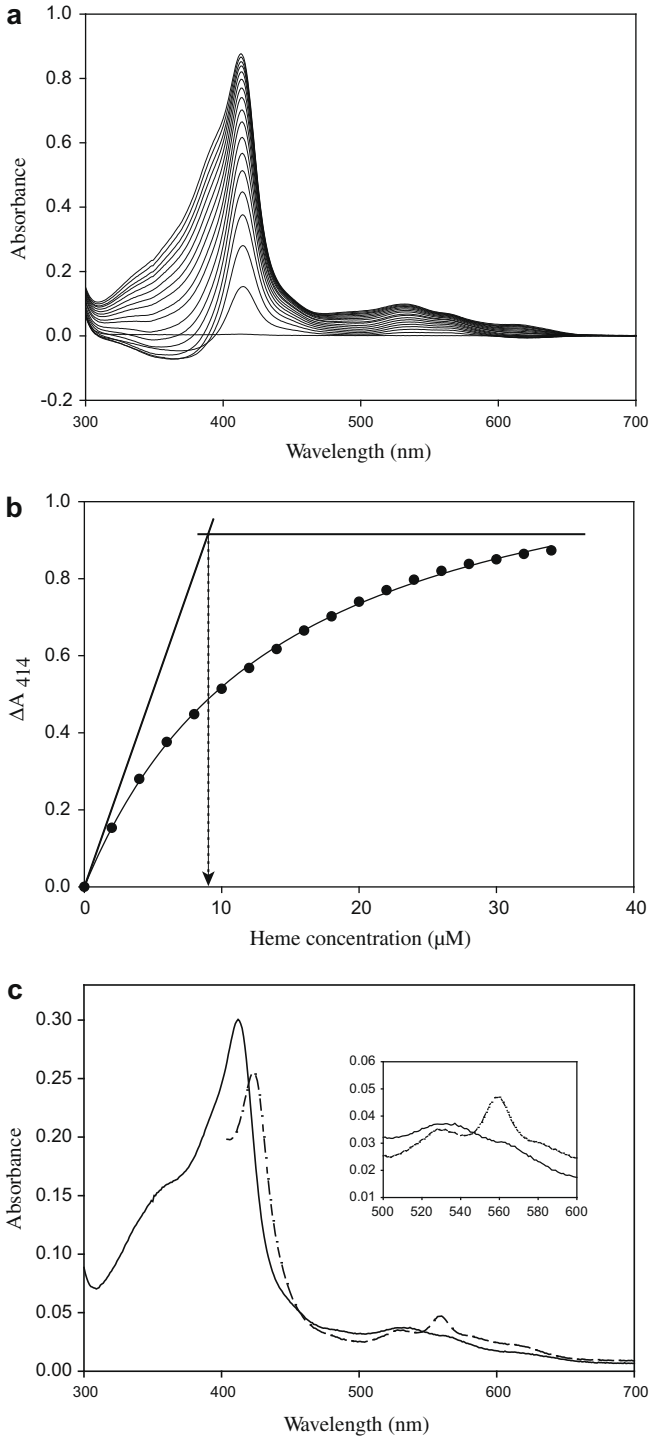

Fig. 2. (A) Difference absorbance spectra of Gpr during titration with heme. Heme was titrated in 2 μM increments up to 34 μM. (B) Heme-binding curve generated from the difference absorbance spectra by plotting ΔA_{414} vs. the heme concentration and fit to a one-binding site quadratic equation. The straight lines represent: (i) the initial slope of the binding curve and (ii) complete binding of heme (ΔA_{414} maximum). A line drawn from their intersection down to the *x*-axis indicates the amount of heme that can bind to Gpr. This vertical line intersects the *x*-axis at close to 8 μM, which is the concentration of Gpr present, indicating a heme binding stoichiometry of 1:1. (C) Absorbance spectrum of the Gpr–heme complex under oxidized (solid) and dithionite-reduced (dashed) conditions. C-terminal strep-tagged Gpr was reconstituted with heme, as described above, and free heme was subsequently removed on a desalting column.

sharp splitting of the α- and β-bands and a shift in the absorbance maxima to 423 (Soret), 528 (β) and 559 nm (α). The Gpr–heme spectrum is similar to the bis-imidazole ligated, low-spin heme in chloroplast b_{559} and in the model compound bis-(*N*-methylimidazole) protoporphyrin IX (Table 1) [19]. The spectrum observed for Gpr–heme is also similar to *E. coli* cytochrome b_{562} and *E. coli* Direct oxygen sensor protein, both of which have a hexacoordinate low-spin heme with axial amino acid ligands comprised of histidine and methionine [15,20]. The absorbance spectrum for Gpr–heme is markedly different than the spectrum of the pentacoordinate high-spin heme found in the oxygen sensing FixL protein of *Bradyrhizobium japonicum* [21].

3.2. Investigation into the heme binding and catalytic activities of human Kvβ2

Gpr shares no homology with known hemoproteins, making identification of the heme binding site difficult; however, the crystal structure of Kvβ, the mammalian homologue, is available. This structure shows a hydrophobic cleft overlying the active site, a structural feature not present in other AKRs (Fig. 3) [7,22]. Notably, MacKinnon and coworkers observed extra unassigned electron density located within this active site cleft in their 2.9 Å resolution structure of a Kv channel in complex with a β-subunit [7]. To test the hypothesis that a similar cleft in Gpr could represent the binding site for heme, we made mutations in Gpr at sites that correspond to regions lining both sides of the hydrophobic cleft observed in the Kvβ2 structure (Fig. 1). Specifically, we deleted residues 100–102 and 254–257 in the native Gpr amino acid sequence. Absorbance spectra of the Δ100–102 and Δ254–257 deletion variants in the presence of heme were identical to heme-bound native Gpr, indicating that these variants are still capable of binding heme in a hexacoordinate low-spin state (Fig. S4). Histidine residues are common heme axial ligands. Thus, in a further attempt to identify residues important for heme binding we replaced amino acid 155 in Gpr, the only histidine residue conserved between Gpr and Kvβ2. Absorbance spectra of the Gpr H155A variant in the presence of heme were also identical to native Gpr (Fig. S4).

The observation that Gpr reversibly associates with heme is intriguing given the significant level of homology observed between Gpr and human Kvβ. Kv channels are rapidly inhibited by hypoxia and the rapid decrease in Kv channel current initiates a cascade of events that ultimately result in increased cardio-respiratory output [23–26]. The identity of the O_2 sensor responsible for the onset of Kv channel inhibition remains unknown, but appears to involve the association of the β-subunit with a functional channel. Kvβ2.1 has been shown to endow Kv4.2 with hemoprotein-like, O_2 sensing characteristics and the hypoxic inhibition of Kvβ2.1 + Kv4.2 currents can be reverted by CO [10]. The only known targets of CO in cellular systems are reduced hemoproteins. Furthermore, the inhibition of Kvβ2.1 + Kv4.2 currents by hypoxia is observed in cell-free patches indicating that freely diffusible cytosolic factors are not responsible for O_2 sensing, but rather that the O_2 sensing machinery is localized to the membrane. It is also known that expression of Kvβ subunits is dramatically greater in the hypoxia-sensitive resistance pulmonary artery smooth muscle cells (PASMC) compared to conduit PASMCs, where hypoxia has little or no effect [27]. Based on these observations, and our own findings with Gpr, we postulated that Kvβ is capable of direct association with heme.

To investigate the possibility that human Kvβ2 is a heme binding protein, we produced a recombinant version of the protein that lacks the N-terminal 35 amino acids, which are known to limit solubility [22]. Difference absorbance spectra of heme titrations performed on C-terminal strep-tagged Kvβ2 gave no indication that the protein has a high affinity, specific interaction with heme (Fig. 4). We attribute the small increases in absorbance observed during the titration to nonspecific interactions of heme with NADPH-bound Kvβ2. We also tested the hypothesis that Kvβ2 is an active L-GAP reductase. Kvβ subunits have high affinity for NADPH and the occupancy of this cofactor is greater than 90% after purification [28]. The catalytic activity of Kvβ can be measured by monitoring the decrease in NADPH absorbance at 363 nm during single-turnover of the enzyme-bound cofactor [8]. At a Kvβ2 concentration of 60 μM in the presence of 10 mM D, L-GAP (5 mM in each enantiomer), 20 mM Tris pH 8.0 and 150 mM KCl, we were unable to observe a decrease in the absorbance of bound NADPH at 363 nm. Thus, we concluded that isolated Kvβ2 does not reduce L-GAP. We confirmed the activity of recombinant human Kvβ2 under these reaction conditions via addition of 5 mM 4-cyanobenzaldehyde, which was consumed with a single-turnover rate of 0.059 min^{-1}. The inability of Kvβ2 to interact with heme *in vitro* or reduce L-GAP may result from the fact that it is not fully assembled with a Kv channel and/or other interacting components. This hypothesis is substantiated by the observation that the Kvβ structure displays an unusual protrusion at the C-terminus of the $(\beta/\alpha)_8$-barrel, which exposes the active site to solvent (Fig. 3) [22]. This unique structural feature suggests that other components may bind to this cleft region to create an active complex. In addition, the observation that Kvβ1.2 endows Kv4.2 with hemoprotein-like O_2-sensitivity, but does not confer this property to *Shaker* channels, provides *in vivo* evidence that certain structural requirements may be necessary to facilitate heme association [10].

Table 1
Absorbance maxima of selected hemoproteins and bis-(*N*-methylimidazole) protoporphyrin IX under oxidizing (Fe(III)) and reducing (Fe(II)) conditions.

Fe(III)				Fe(II)		
Sample	Soret, γ	β	α	Soret, γ	β	α
Gpr	412	528	564	423	528	559
His, His axial ligands (6c-LS)						
cyt b_{559}	413	534	562	427	530	559
$PPIX(Im)_2$	413	535	564	426	530	559
His, Met axial ligands (6c-LS)						
Dos	416	530	564	427	532	563
cyt b_{562}	418	530	564	427	531	562
His axial ligand (5c-HS)						
*Bj*FixL	395	509	645	437	556	

4. Discussion

The discovery that Gpr co-purifies with heme from crude cell extracts strongly suggests that this prosthetic group participates in its physiological function. A functional link between O_2-sensitivity and Gpr activity is suggested by the discovery that *gpr* transcription is regulated by FNR, an oxygen-responsive global regulator of gene expression that governs the response of *E. coli* to altered O_2 levels [29]. One possibility is that the heme cofactor plays a regulatory role in Gpr function. Indeed, several heme-based sensor proteins have been recently described, which modulate the activity of an associated ligand binding/catalytic site in response to the reversible association of a gas with the heme in the sensory domain [20,21,30]. In addition, *Gpr* clusters with a family of putative monooxygenases in the following organisms; *Acinetobacter* sp. *ADP1*, *Mycobacterium* sp. *MCS*, *Pseudomonas fluorescens* Pf0-1, *Rhodococcus jostii* RHA1, and *Xanthomonas axonopodis* pv. citri strain 306 (V. de Crecy-Lagard, personal communication), raising the pos-

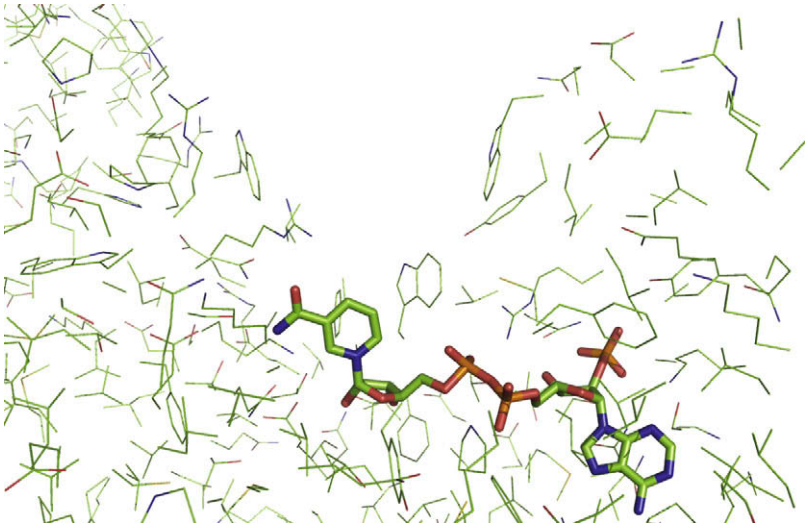

Fig. 3. Crystal structure of *H. sapien* Kvβ2 depicting the hydrophobic cleft located above the bound $NADP^+$ cofactor. Image was constructed with PyMol and PDB entry 1QRQ.

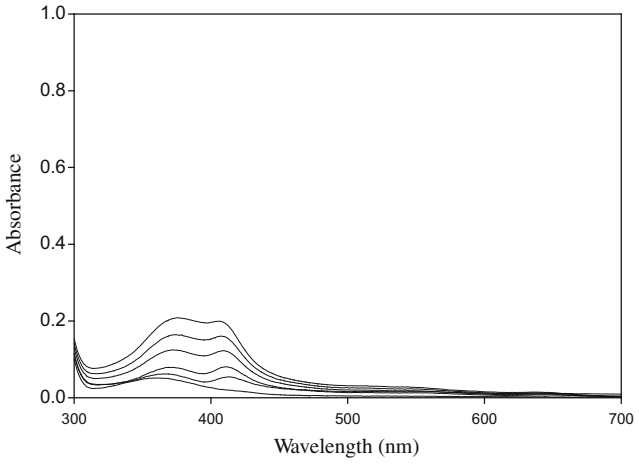

Fig. 4. Difference absorbance spectra of 8 μM *H. sapien* Kvβ2 during titration with heme in 2 μM increments up to 10 μM.

sibility that Gpr performs a heme-dependent, monooxygenase-like function *in vivo* [31].

The L-GAP reductase activity of Gpr does not require heme. This finding raises the question of whether L-GAP reduction is the true physiological function of this enzyme or whether it represents a conditionally advantageous promiscuous function. The high catalytic efficiency of L-GAP reduction ($4.2 \times 10^5\ M^{-1}\ s^{-1}$) supports the notion that this chemical reaction is a physiologically relevant role of Gpr. It is possible that Gpr possesses multiple functions *in vivo*, only some of which are linked to the observed heme binding abilities reported herein. Further experiments will be necessary to establish the functional significance of the association between heme and Gpr.

Appendix A. Supplementary material

Supplementary data associated with this article can be found, in the online version, at doi:10.1016/j.bioorg.2009.11.003.

References

[1] K.K. Desai, B.G. Miller, Biochemistry 47 (2008) 7983–7985.
[2] J.P. Richard, ACS Chem. Biol. 3 (2008) 605–607.
[3] C.T. Tang, R. Engel, B.E. Tropp, Agents Chemother. 11 (1977) 147–153.
[4] G. Leoncini, M. Maresca, S. Ronchi, A. Bonsignore, Ital. J. Biochem. 28 (1979) 232–244.
[5] E.M. Ellis, FEMS Microbiol. Lett. 216 (2002) 123–131.
[6] J. Rettig, S.H. Heinemann, F. Wunder, C. Lorra, D.N. Parcej, J.O. Dolly, O. Pongs, Nature 369 (1994) 289–294.
[7] S.B. Long, E.B. Campbell, R. MacKinnon, Science 309 (2005) 897–903.
[8] J. Weng, Y. Cao, N. Moss, M. Zhou, J. Biol. Chem. 281 (2006) 15194–15200.
[9] Y. Pan, J. Weng, Y. Cao, R. Bhosle, M. Zhou, J. Biol. Chem. 283 (2008) 8634–8642.
[10] M.T. Perez-Garcia, J.R. Lopez-Lopez, C. Gonzalez, J. Gen. Physiol. 113 (1999) 897–907.
[11] J.-H. Fuhrhop, K.M. Smith, in: K.M. Smith (Ed.), Porphyrins, Elsevier, Amsterdam, 1975, pp. 757–868.
[12] I. Kirschner-Zilber, E. Rabizadeh, N. Shaklai, Biochim. Biophys. Acta. 690 (1982) 20–30.
[13] L. Yi, S.W. Ragsdale, J. Biol. Chem. 282 (2007) 21056–21067.
[14] M. Kitagawa, T. Ara, M. Arifuzzaman, T. Ioka-Nakamichi, E. Inamoto, H. Toyonaga, H. Mori, DNA Res. 12 (2005) 291–299.
[15] E. Itagaki, L.P. Hager, J. Biol. Chem. 241 (1966) 3687–3695.
[16] A. Wilks, P.R. Ortiz de Montellano, J. Sun, T.M. Loehr, Biochemistry 35 (1996) 930–936.
[17] M.D.L. Suits, J. Lang, G.P. Pal, M. Couture, Z. Jia, Protein Sci. 18 (2009) 825–838.
[18] E.P. Skaar, A.H. Gaspar, O. Schneewind, J. Biol. Chem. 279 (2004) 436–443.
[19] G.T. Babcock, W.R. Widger, W.A. Cramer, W.A. Oertling, J.G. Metz, Biochemistry 24 (1985) 3638–3645.
[20] V.M. Delgado-Nixon, G. Gonzalez, M.A. Gilles-Gonzalez, Biochemistry 39 (2000) 2685–2691.
[21] M.A. Gilles-Gonzalez, G. Gonzalez, M.F. Perutz, Biochemistry 33 (1994) 8067–8073.
[22] J.M. Gulbis, S. Mann, R. MacKinnon, Cell 97 (1999) 943–952.
[23] J. Lopez-Barneo, J.R. Lopez-Lopez, J. Urena, C. Gonzalez, Science 241 (1988) 580–582.
[24] M.D. Ganfornina, J. Lopez-Barneo, Proc. Natl. Acad. Sci. USA 88 (1991) 2927–2930.
[25] C. Jiang, G.G. Haddad, J. Physiol. 481 (1994) 15–26.
[26] J.R. Lopez-Lopez, C. Gonzalez, FEBS Lett. 299 (1992) 251–254.
[27] E.A. Coppock, M.M. Tamkun, Am. J. Physiol. Lung Cell Mol. Physiol. 281 (2001) L1350–L1360.
[28] S.Q. Liu, H. Jin, A. Zacarias, S. Srivastava, A. Bhatnagar, J. Biol. Chem. 276 (2001) 11812–11820.
[29] Y. Kang, K.D. Weber, Y. Qiu, P.J. Kiley, F. R Blattner, J. Bacteriol. 187 (2005) 1135–1160.
[30] M.A. Gillez-Gonzalez, G. Gonzalez, J. Inorg. Biochem. 99 (2005) 1–22.
[31] I.M. Keseler, J. Collado-Vides, S. Gama-Castro, J. Ingraham, S. Paley, I.T. Paulsen, M. Peralta-Gil, P.D. Karp, Nucl. Acids Res. 33 (2005) D334–D337.